CHEMICAL ENGINEERING TRANSACTIONS
VOL. 122, 2025
A publication of AIDIC
The Italian Association of Chemical Engineering
Online at www.cetjournal.it
Guest Editors: Jeng Shiun Lim, Bohong Wang, Guo Ren Mong, Petar S. Varbanov

ISBN 979-12-81206-23-6; **ISSN** 2283-9216
DOI: 10.3303/CET25122077

Computational Fluid Dynamics Analysis of Ammonia (NH_3) Selective Catalytic Reduction in Semicircular Ring-baffled Fluidized Bed Reactor

Brylle Reovince Rosales*, Daniela Bag-ao, John Ogad, Christine Cabrera

Mapúa Malayan Colleges Laguna, Cabuyao City, Laguna, Philippines, 4025
brarosales@mcl.edu.ph

This study utilized an unsteady multiphase Computational Fluid Dynamics model in ANSYS FLUENT 2024 R2 to investigate the impact of semicircular baffles on the hydrodynamics and NO_x removal efficiency in a fluidized bed reactor. Both standard and fast Selective Catalytic Reduction mechanisms were considered in the reactor employing the CuO/γ-Al_2O_3 as catalyst. The baffle-free reactor (FFB) model was validated against experimental data through mesh optimization, and kinetic parameter calibration. Subsequently, systematic simulations of 27 baffled configurations (single, double, and triple baffles) demonstrated significant improvements in NO reduction. At 300 °C, configurations DB3, TB6, and TB14 generated the highest conversions of 93.20 %, 93.33 %, and 93.12 %, respectively. Notably, at 250 °C, these configurations maintained high efficiencies suggesting that the addition of baffles could replicate the performance of FFB even at a lower temperature. The study revealed that the semicircular baffles increased the solid holdup, radial gas velocity, and granular temperature, thereby enhancing gas–solid interactions.

1. Introduction

Despite the accelerating global shift toward renewable energy, fossil fuels remain deeply entrenched in the global energy landscape as projected by the U.S. Energy Information Administration (Chen et al., 2021). Since the 1990s, fossil fuel combustion has contributed the vast majority of NO_x emissions worldwide—about 95% globally, 90% in Europe, 88% in East Asia, and 96% in North America (Song, 2021). Among available control strategies, ammonia selective catalytic reduction (NH_3-SCR) is widely recognized as the most efficient industrial method for NO_x treatment (Zhang et al., 2021). While the NH_3-SCR process involves multiple reaction pathways, NO_x in flue gas typically contains ~95 % NO and ~5 % NO_2 (Gholami et al., 2020), making the Standard SCR and Fast SCR reactions the most relevant as shown in Eq(1) and Eq(2), respectively:

$$4NO + 4NH_3 + O_2 \rightarrow 4N_2 + 6H_2O \quad (1)$$

$$NO + 2NH_3 + NO_2 \rightarrow 2N_2 + 3H_2O \quad (2)$$

Industrial-scale NH_3-SCR systems typically employ honeycomb monolith reactors due to their mechanical robustness. However, fluidized bed reactors offer distinct advantages for treating flue gas with high dust loading: superior gas–solid contact, improved NO_x reduction efficiency, and the ability for in-situ catalyst regeneration (Cheng and Bi, 2014). Hossain et al. (2022) indicated that fluidized bed gasifier provides additional features such as even temperature distribution, lower residence time, and short heat up period. The CuO/γ-Al_2O_3 catalyst was selected in this study due to its low attrition index and high removal efficiency in simultaneous treatment NO_x and SO_x (Rahmanenijad et al., 2012). Nonetheless, fluidized bed reactor performance can be hindered by challenges such as increased bubble size and solids back-mixing (Cheng and Bi, 2014). Recent studies have sought to mitigate these limitations through internal reactor modifications. Benzarti et al. (2021) reported that semicircular and trapezoidal baffles enhanced heat and mass transfer in circulating fluidized bed risers, minimized wall backflow, and promoted both axial and radial mixing. Similarly, De Felice et al. (2024)

Paper Received: 5 August 2025; Revised: 20 September 2025; Accepted: 27 September 2025
Please cite this article as: Rosales B.R., Bag-ao D., Ogad J., Cabrera C., 2025, Computational Fluid Dynamics Analysis of Ammonia (NH_3) Selective Catalytic Reduction in Semicircular Ring-baffled Fluidized Bed Reactor, Chemical Engineering Transactions, 122, 457-462 DOI:10.3303/CET25122077

demonstrated that introducing baffles improves fluidization stability and quality. Rosales and Mendoza (2025) further showed that rectangular ring baffles increased solids holdup and radial gas velocity, improving gas–solid interaction even at lower operating temperatures. However, the simultaneous removal of NO and NO_2 in a baffled fluidized bed reactor was not yet investigated in the literature.

This work examines the influence of semicircular (semi-toroidal in 3D) ring baffles on NH_3-SCR performance in a fluidized bed reactor using CFD simulations. Experimental data from Irfan et al. (2009) were used to validate the simulation framework. Extending from Rosales and Mendoza (2025) works, this research aims to evaluate how varying semicircular baffle configurations affect reactor hydrodynamics and NO_x removal efficiency. The simulations tracked solids volume fraction and back-mixing to provide insight into the gas–solid interaction.

2. Research Methodology

2.1 Conceptual Framework

The methodology, adapted from Rosales and Mendoza (2025) and outlined in Figure 1, involved CFD simulations of the baffle-free (FFB) reactor validated against Irfan et al. (2009). Mesh independence and kinetic calibration were performed to ensure accuracy. The validated model was then used to assess semicircular baffles under identical baseline conditions. NO_x removal efficiencies were compared using Welch's ANOVA, and axial profiles of NO mass fraction, solids holdup, and radial gas velocity were examined to characterize reactor hydrodynamics.

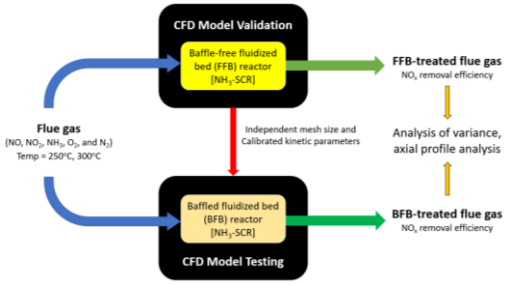

Figure 1: Conceptual framework of the present study

2.2 Geometry and meshing of reactor

The reactor was modeled with a height of 0.6 m and diameter of 0.1 m. A 2D domain was adopted for faster computation without major accuracy loss (Oliveira and Vianna, 2022). Although 2D simulations differ from 3D, proper choice of specularity, restitution, and grid resolution can produce results consistent with experiments (Shi et al., 2019). Figure 2a shows the FFB geometry and mesh, using 0.0025 m quadratic elements. Mesh independence was checked with coarser (0.005 m) and finer (0.001 m) grids, evaluated by bubble diameter, NO removal efficiency, and computation time over 20 s of flow. Figure 2b illustrates the baffled fluidized bed (BFB) setup, where inlet-baffle and inter-baffle distances were defined relative to baffle centers.

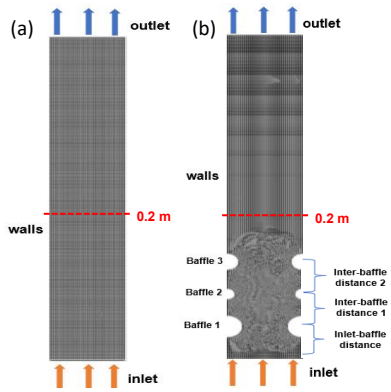

Figure 2: Mesh of (a) FFB model; (b) BFB model

2.3 Fluidized bed reactor simulations

Simulations were run in transient mode using ANSYS FLUENT 2024 R2 on a laptop (Intel® Core™ i7, 16 GB RAM). The baseline FFB case used $u_g = 2u_{mf}$ (u_{mf} = 0.049 m/s), 300 °C, and inlet concentrations of 400 ppm NO, 21.05 ppm NO_2, and 600 ppm NH_3. Catalyst properties adapted from Rahmaninejad et al. (2012), included 220 µm particles, density of 2116.6 kg/m³, 0.2 m bed height, and void fraction of 0.42. Outlet NO and NO_2 mass fractions were validated against experiments. Eulerian–Eulerian framework with Syamlal–O'Brien drag model and the Realizable k-ε model was applied. Governing equations for mass, momentum, energy, and species followed the formulations described in Xing et al. (2021). First-order upwind discretization and a convergence criterion of 1 x 10^{-3} were used to handle multiphase complexity (Tong et al., 2023).

3. Results and Discussion

3.1 Model validation and kinetic parameter calibration

The FFB reactor model was validated by comparing the simulated bubble diameter and NO removal efficiency with the experimental findings of Irfan et al. (2009). As shown in Figure 3, all tested mesh sizes produced bubble diameters consistent with the experimental data for both U_{mf} and U_g, with the medium mesh (0.0025 m) giving results closest to the measurements (RMSE = 0.00307). Moreover, Figure 4 reveals that this mesh size reproduced the experimental hydrodynamic behavior more accurately than either the coarser or finer grids. This eliminates both the 0.005 m and 0.001 m element sizes as option. Usually, finer mesh generates higher accuracy but this deviation may be linked to the added complexity of multiphase reaction interactions at smaller cell sizes, as also noted by Rosales and Mendoza (2025). Furthermore, computational efficiency was significantly affected by mesh size: for a simulated flow time of 20 s, the medium mesh required only 32 min, compared to 121 min for the finer mesh. Given that both meshes yielded comparable accuracy but with substantial differences in computational cost, 0.0025 m grid was selected for all subsequent FFB simulations.

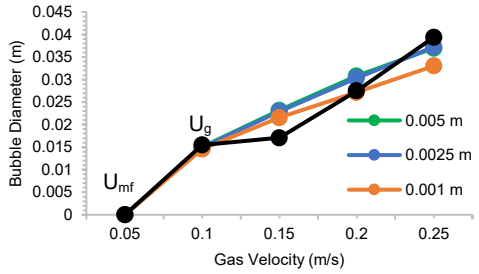

Figure 3: Bubble diameter comparison for mesh independence test

Following mesh selection, kinetic parameters were calibrated using only the standard-SCR reaction to align the model with the original work of Irfan et al. (2009), which did not include NO_2 in the simulated flue gas composition. In their study, the standard-SCR was described as a first-order reaction in NO following the Eley–Rideal mechanism, with rate constants of 1.77 s^{-1} and 2.3 s^{-1} at 250 °C and 300 °C, respectively, corresponding to NO removal efficiencies of 86 % and 90 %. Direct implementation of the Arrhenius equation derived from these constants resulted in NO removal efficiencies exceeding 99 % at 300 °C. To address this, alternative kinetic parameters were tested to refine the Arrhenius equation, following the approach similar to the oxidative dehydrogenation study of Mendoza and Hwang (2018). The calibrated Arrhenius equation, described in Eq(3), yielded results of 86.51 % and 90.03 % NO removal efficiencies for 250 °C and 300 °C, respectively. This is relatively close to the calibrated equation used by Rosales and Mendoza (2025) which integrates adsorption and diffusion effects into a unified parameter.

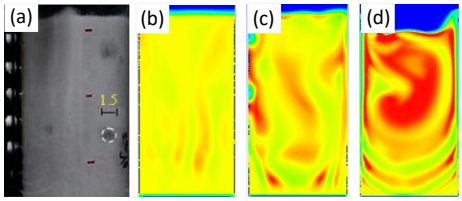

Figure 4: Snapshots of solids volume fraction of (a) Experimental reactor [Adapted from Figure 4 with permission from Irfan et al. Copyright 2009 American Chemical Society]; (b) 0.005 m mesh; (c) 0.0025 m mesh; (d) 0.001 m mesh

For the fast-SCR pathway, since there is no experimental data available for calibration, the reaction was modeled as second-order in both NO and NO_2, as described by Li et al. (2021), and expressed in Eq(4).

$$k_{standard} = 2.9758\ s^{-1}\ e^{\frac{-8.7917\times10^{6}\frac{J}{kgmol}}{RT}} \quad (3)$$

$$k_{fast} = 3.96\times10^{16}\ \frac{m^3}{kgmol\cdot s}\ e^{\frac{-89.6\times10^{6}\frac{J}{kgmol}}{RT}} \quad (4)$$

3.2 Baffled fluidized bed (BFB) reactor simulations

Following the calibration of the FFB reactor, baffles were incorporated to evaluate their influence under baseline operating conditions. The different baffle arrangements, summarized in Table 1, were classified according to the number of baffles used: single-baffle (SB), double-baffle (DB), and triple-baffle (TB). For all configurations, baffles were positioned within a vertical span of 0.2 m to maximize particle–baffle interaction. Adjustments to the bed height were made to compensate for the volume occupied by the baffles, ensuring that the overall catalyst mass remained constant across cases.

Table 1: FFB and BFB simulations

Geometry Name	Baffle 1 (radius, m)	Baffle 2 (radius, m)	Baffle 3 (radius, m)	Inlet-baffle distance, m	Inter-baffle distance 1, m	Inter-baffle distance 2, m	Time-averaged Turbulent Kinetic Energy (J/kg)	NO removal efficiency (%)	NO_2 removal efficiency (%)
FFB	-	-	-	-	-	-	0.0169	90.75	99.97
SB1	0.01	-	-	0.09	-	-	0.0182	90.30	99.97
SB2	0.015	-	-	0.085	-	-	0.1730	90.43	99.97
SB3	0.02	-	-	0.08	-	-	0.0186	90.66	99.97
DB1	0.01	0.01	-	0.09	0.08	-	0.0175	90.25	99.97
DB2	0.015	0.015	-	0.085	0.07	-	0.2960	91.57	99.97
DB3	0.02	0.02	-	0.08	0.06	-	0.0216	93.20	99.97
DB4	0.01	0.015	-	0.09	0.075	-	0.2110	91.13	99.97
DB5	0.015	0.01	-	0.085	0.075	-	0.0192	90.77	99.97
DB6	0.01	0.02	-	0.09	0.07	-	0.0304	92.63	99.97
DB7	0.02	0.01	-	0.08	0.07	-	0.0177	92.15	99.97
DB8	0.02	0.015	-	0.08	0.065	-	0.1770	92.64	99.97
DB9	0.015	0.020	-	0.085	0.065	-	0.0241	92.17	99.97
TB1	0.01	0.01	0.01	0.05	0.04	0.04	0.0157	89.93	99.97
TB2	0.015	0.015	0.015	0.045	0.03	0.03	0.0201	91.90	99.97
TB3	0.02	0.02	0.02	0.04	0.02	0.02	0.0199	92.83	99.97
TB4	0.01	0.015	0.02	0.05	0.035	0.025	0.0185	92.27	99.97
TB5	0.01	0.02	0.015	0.05	0.03	0.025	0.0183	92.84	99.97
TB6	0.02	0.01	0.015	0.04	0.03	0.035	0.0191	93.33	99.97
TB7	0.02	0.015	0.01	0.04	0.025	0.035	0.0191	92.29	99.97
TB8	0.015	0.01	0.02	0.045	0.035	0.03	0.0169	92.63	99.97
TB9	0.015	0.02	0.01	0.045	0.025	0.03	0.0188	93.06	99.97
TB10	0.01	0.015	0.015	0.05	0.035	0.03	0.0169	92.44	99.97
TB11	0.01	0.02	0.02	0.05	0.03	0.02	0.0216	92.37	99.97
TB12	0.015	0.01	0.01	0.045	0.035	0.04	0.0203	91.00	99.97
TB13	0.015	0.02	0.02	0.045	0.025	0.02	0.0211	92.86	99.97
TB14	0.02	0.015	0.015	0.04	0.025	0.03	0.0169	93.12	99.97
TB15	0.02	0.01	0.01	0.04	0.03	0.04	0.0155	92.04	99.97

The calibrated FFB attained an NO removal efficiency of 90.75 %, which is marginally higher than the 90.03 % recorded in the kinetic calibration stage. This improvement is likely linked to the presence of NO_2 in the inlet gas stream, which activates the fast-SCR mechanism. Because both the standard-SCR and fast-SCR pathways consume NO, their combined effect resulted in enhanced NO conversion. As shown in the table 1, the

introduction of baffles produced a notable impact on bed hydrodynamics and gas–solid interaction patterns, as confirmed by Welch's ANOVA ($p = 5.9 \times 10^{-6}$). The 27 baffled configurations averaged 91.96% NO removal, versus 90.75% for the baffle-free reactor. This modest 1.2-point gain translates to a 13% reduction in residual NO, underscoring its environmental significance. The best case, TB6 (93.33%), achieved a 28% reduction in residual NO relative to the baseline. In contrast, NO_2 removal efficiencies were essentially unchanged across all scenarios, suggesting that the fast-SCR process is largely unaffected by changes in fluidization dynamics. Finally, the data in Table 1 indicate that higher turbulence intensity (e.g. DB2 and DB4) did not necessarily lead to faster NO depletion, as also reported by Guo et al. (2023) and validated by Rosales and Mendoza (2025).

Among all tested arrangements, TB14, DB3, and TB6 achieved the highest NO removal rates (>93 %), in ascending order. These designs generated larger turbulent eddies compared with the FFB, shown in Figure 5, thereby improving gas–solid contact efficiency. Compared to the results reported by Rosales and Mendoza (2025), the performance gains in this study can be linked to the semi-toroidal baffle design, which offers a smoother, continuous curvature unlike rectangular baffles. This shape appears to limit resistance to radial mixing while promoting an axial flow pattern and to generate axially stable eddies, consistent with the trends observed by Benzarti et al. (2021) as shown in Figure 6. Furthermore, the incorporation of ring baffles enhanced solids holdup and promoted radial mixing in the zones located between and after the baffles. This improvement showed a direct correlation with the NO depletion observed along the reactor length, as illustrated in Figure 7. These trends are in agreement with the observations reported by Benzarti et al. (2021).

After assessing the different baffle configurations under baseline conditions, the study examined their performance at a lower operating temperature of 250 °C, following the methodology of Irfan et al. (2009). The NO removal efficiencies obtained for DB3, TB6, and TB14 were 89.56 %, 90.24 %, and 89.80 %, respectively. These values align with trends reported in the literature and can be linked to the increase in granular temperature of the solid catalysts, as discussed by Rosales and Mendoza (2025). The findings reinforce that the use of semicircular ring baffles enhances gas–solid mixing and prolongs contact time, which in turn elevates the granular temperature and contributes to higher NO removal efficiency.

4. Conclusions

The unsteady multiphase CFD analysis demonstrated that integrating semicircular ring baffles into a fluidized bed reactor significantly improves hydrodynamics and NO_x removal efficiency. The validated FFB model enabled evaluation of 27 baffled configurations, with DB3, TB6, and TB14 achieving more than 93% NO conversion at 300 °C and sustaining high efficiencies at 250 °C. Performance gains were driven by increased solids holdup, elevated radial gas velocity, and higher granular temperature, improving the gas–solid interaction. Semicircular baffles thus represent an effective design modification for SCR reactors. Future studies should consider higher NO_x loads, dust entrainment, and side reactions.

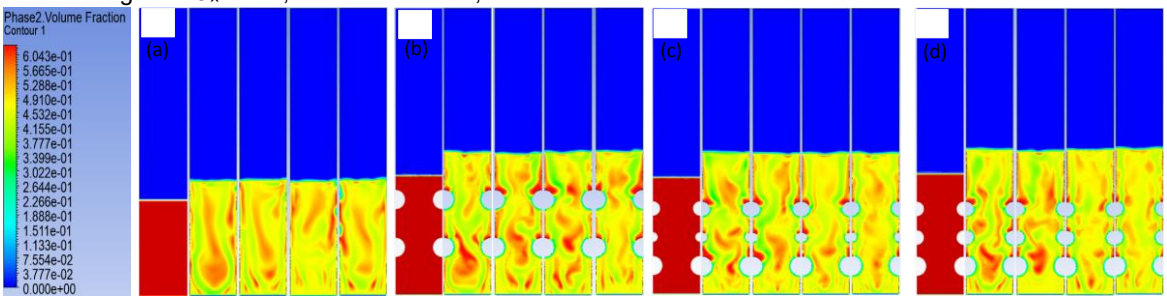

Figure 5: Snapshots of solids volume fraction at t = 0 s, 5 s, 10 s, and 20 s: (a) FFB; (b) DB3; (c) TB6; (d) TB14

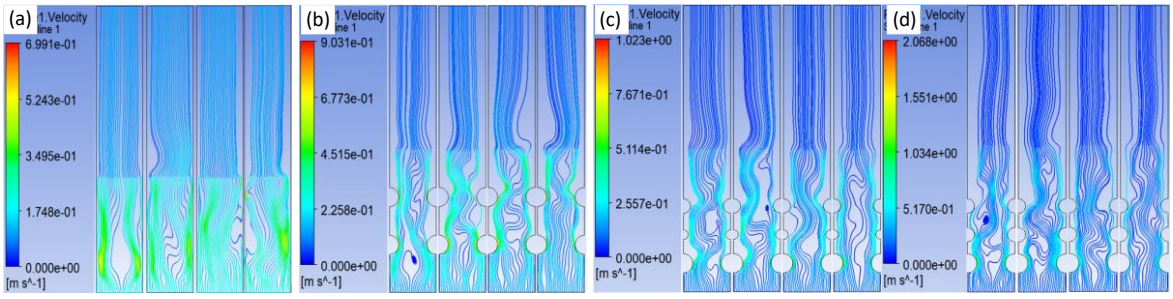

Figure 6: Snapshots of gas velocity at t = 5 s, 10 s, and 20 s: (a) FFB; (b) DB3; (c) TB6; (d) TB14

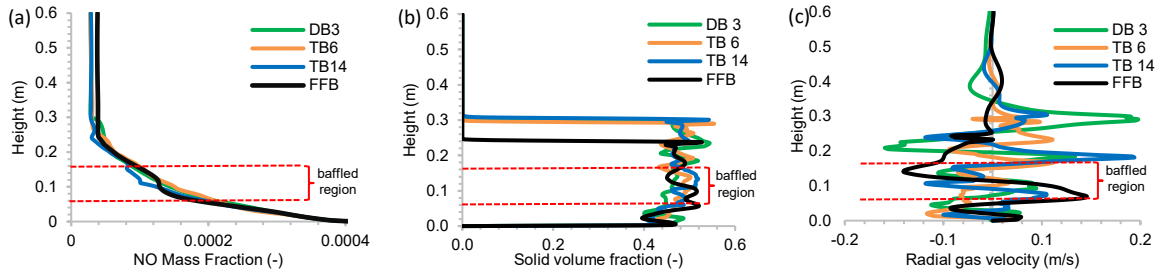

Figure 7: Analysis of FFB, DB3, TB6, and TB14 configurations in axial direction: (a) NO mass fraction; (b) solid volume fraction; (c) radial gas velocity

References

Benzarti S., Mhiri H., Bournot H., 2021, Numerical simulation of baffled circulating fluidized bed with Geldart B particles, Powder Technology, 380, 629–637.

Chen R., Zhang T., Guo Y., Wang J., Wei J., Yu Q., 2021, Recent advances in simultaneous removal of SO2 and NOx from exhaust gases: Removal process, mechanism and kinetics, Chemical Engineering Journal, 420, 127588.

Cheng X., Bi X. T., 2014, A review of recent advances in selective catalytic NOx reduction reactor technologies, Particuology, 16, 1–18.

De Felice G., Li S., Chung Y., Canals Busqueta J., Ma Z., Gallucci F., Rebrov E., 2025, Vertical baffles in a fluidized bed reactor: Hydraulic assessment with a numerical and experimental approach, Chemical Engineering Science, 302, 120805.

Gholami F., Tomas M., Gholami Z., Vakili M., 2020, Technologies for the nitrogen oxides reduction from flue gas: A review, Science of The Total Environment, 714, 136712.

Guo Q., Dai E., Xu S., Yang Y., Yang N., Xie G., Nie Z., 2023, Numerical simulation of fluidization behavior and chemical performance for hydrochlorination of silicon tetrachloride in a fluidized bed reactor. Processes, 11(10), 2979.

Hossain M., Kumar D., Paul N., Rahman S., Rahman M., Uddin M., Pirozzi D., Uddin M., Yousuf A., 2022, Design and Development of Bubbling Fluidized Bed Gasifier for Non-Woody Biomass Gasification, Chemical Engineering Transactions, 92, 289-294.

Irfan M. F., Kim S. D., Usman M. R., 2009, Modeling of NO removal over CuO /γ-Al2O3 catalyst in a bubbling fluidized bed reactor, Industrial Engineering Chemistry Research, 48(17), 7959–7964.

Li S., Zhang C., Zhou A., Li Y., Yin P., Mu C., Xu J., 2021, Experimental and kinetic modeling study for N2O formation of NH3-SCR over commercial Cu-zeolite catalyst, Advances in Mechanical Engineering, 13(4).

Mendoza J. A., Hwang S., 2018, Tubular reactor design for the oxidative dehydrogenation of butene using computational fluid dynamics (CFD) modelling, Korean Journal of Chemical Engineering, 35(11), 2157–2163.

Oliveira M., Vianna S., 2022, Evaluating the Influence of the Leak Reynolds Numbers on the Behavior of Underwater Gas Plumes: a CFD Study, Chemical Engineering Transactions, 91, 559-564

Rahmaninejad F., Gavaskar V. S., Abbasian J., 2012, Dry regenerable CuO/ ϒ-Al2O3 catalyst for simultaneous removal of SOx and NOx from flue gas. Applied Catalysis B: Environmental, 119–120, 297–303.

Rosales B. R., Mendoza J. A., 2025, Effect of ring baffles in simulated flue gas denitrification via NH3-SCR in fluidized bed reactor: A CFD approach, Journal of Physics: Conference Series, 2947(1), 012009, Barcelona, Spain.

Shi H., Komrakova A., & Nikrityuk P., 2019, Fluidized beds modeling: Validation of 2D and 3D simulations against experiments, Powder Technology, 343, 479–494.

Song W., Liu X.Y., Hu C.C., Chen G.Y., Liu X.J., Walters W. W., Michalski G., Liu C.Q., 2021, Important contributions of non-fossil fuel nitrogen oxides emissions, Nature Communications, 12(1).

Tong S., Miao B., Zhang W., Zhang L., Chan S. H., 2023, Optimization of methane catalytic decomposition in a fluidized bed reactor: A computational approach, Energy Conversion and Management, 297, 117719.

Xing X., Zhang C., Jiang B., Sun Y., Zhang L., Briens C., 2021, Effect of a baffle on bubble distribution in a bubbling fluidized bed, Processes, 9(7), 1150.

Zhang W., Chen J., Guo L., Zheng W., Wang G., Zheng S., Wu X., 2021, Research progress on NH3-SCR mechanism of metal-supported zeolite catalysts, Journal of Fuel Chemistry and Technology, 49(9), 1294–1315.